

Full length article

## Phase-dependent velocity selective coherent population trapping in a folded three-level ( $\Lambda$ ) system under standing wave excitation

M.S. Shahrar<sup>a</sup>, P.R. Hemmer<sup>b</sup>, M.G. Prentiss<sup>c</sup>, A. Chu<sup>c</sup>, D.P. Katz<sup>d</sup> and N.P. Bigelow<sup>e</sup>

<sup>a</sup> Research Laboratory of Electronics, Massachusetts Institute of Technology, Cambridge, MA 02139, USA

<sup>b</sup> Rome Laboratory/EROP, Hanscom AFB, MA 01731 USA

<sup>c</sup> Department of Physics, Harvard University, Cambridge, MA 02138, USA

<sup>d</sup> Division of Applied Sciences, Harvard University, Cambridge, MA 02138, USA

<sup>e</sup> Department of Physics and Astronomy and the Laboratory for Laser Energetics, University of Rochester, Rochester, NY 14627, USA

Received 23 February 1993; revised manuscript received 17 June 1993

Theoretically identified are the conditions under which velocity selective coherent population trapping (VSCPT) takes place when a three-level  $\Lambda$  system is excited by a pair of Raman resonant standing waves. The efficiency of the VSCPT depends on the relative phase,  $\phi$ , between the standing waves, and vanishes when  $\phi=0$ . Also reviewed are previous experimental observations by Aspect et al. [Phys. Rev. Lett. 61 (1988) 826] which qualitatively validate the predictions. Finally, the implication of this result to the feasibility of a dense trap of sub-recoil temperature  $\Lambda$  atoms is discussed.

### 1. Introduction

Recently, there has been a great deal of interest in the forces experienced by a folded three-level ( $\Lambda$ ) atom. Aspect et al. [1] first demonstrated that such an atom can be cooled below the recoil limit via velocity selective coherent population trapping (VSCPT), when excited by a pair of counter-propagating travelling waves. In this paper, we show that VSCPT occurs in a  $\Lambda$  atom excited by a pair of Raman resonant standing waves, and its efficiency depends on the relative phase<sup>#1</sup>,  $\phi$ , between the standing waves. We will also review previous experimental observations made by Aspect et al. [1] in Raman resonant standing waves which are consistent with our theoretical predictions. Finally, we briefly describe the generalization of VSCPT in standing waves to three dimensions [3].

The interest in VSCPT in Raman resonant standing waves stems from our earlier experimental [4] observation of deflection and cooling of  $\Lambda$  sodium atoms in an atomic beam. This experiment suggests that these standing wave forces could be used to design a stimulated force trap [4]. In addition, we have developed a theory [3] which predicts that the cooling can be made to have characteristics very similar to those of conventional polarization gradient (pol-grad) cooling, so that such a trap should have a sub-Doppler temperature. The results derived in the present paper suggest that it may be possible to reach a sub-recoil temperature in a Raman force trap.

The existence of VSCPT corresponds to absence of diffusion for zero velocity atoms in the trapped state. However, Chang et al. [5] have previously computed a non-zero diffusion coefficient in Raman resonant standing waves by a perturbative numerical solution of the Wigner density matrix equation of motion. Our disagreement with Chang et al. seems to stem from the fact that they assumed, a priori, that the distribution of atoms in momentum space is smooth, which is in sharp contrast with the result of VSCPT.

<sup>#1</sup> Mauri et al. [2] also found a process of VSCPT with a phase-dependent efficiency.

## 2. Theory of standing wave VSCPT

In general, it is rather difficult to find an ideal  $\Lambda$  system. One example is when a  $j=1 \leftrightarrow j'=1$  transition is excited by a pair of left- and right-circularly polarized waves, which turns into a  $\Lambda$  system after a few optical pumping cycles [1]. This is illustrated in fig. 1a, for the case where each circular polarization forms a standing wave. The lines joining the magnetic sublevels indicate the allowed electric-dipole transitions. As can be seen, the  $m=0 \leftrightarrow m'=0$  transition is not allowed. In addition, the fields do not excite any  $\pi$  transitions (the dashed lines). As a result, after a few spontaneous lifetimes, the atoms originally in the  $m=0$  sublevel get completely depleted, and we get a perfect  $\Lambda$  system, as indicated by the thick lines. In the coming analysis, we will use this  $j=1 \leftrightarrow j'=1$  system. We emphasize, however, that the analysis is valid for any ideal  $\Lambda$  system, independent of the polarizations of the excitation fields.

The three atomic states  $|a\rangle$ ,  $|b\rangle$ , and  $|c\rangle$  in fig. 1b correspond respectively to the  $m=-1$ ,  $m=+1$ , and  $m'=0$  states. The electric field is expressed as

$$E = \frac{1}{2} E_1(z) [\exp(-i\omega_1 t) + \text{c.c.}] + \frac{1}{2} E_2(z) [\exp(-i\omega_2 t) + \text{c.c.}] , \quad (1)$$

where

$$E_1(z) = \hat{\sigma}_+ E_{10} \cos(k_1 z) , \quad E_2(z) = \hat{\sigma}_- E_{20} \cos(k_2 z + \phi) , \quad (2)$$

$z$  is the position of the center of mass of the atom,  $\phi$  is the phase difference between the standing waves, and  $\hat{\sigma}_+$  and  $\hat{\sigma}_-$  are the polarization vectors, corresponding respectively to right- and left-circular polarizations. We define the Rabi frequencies as

$$g_1(z) \equiv \mu_{ac} \cdot E_1 / \hbar \equiv g_{10} \cos(k_1 z) , \quad g_2(z) \equiv \mu_{bc} \cdot E_2 / \hbar \equiv g_{20} \cos(k_2 z + \phi) . \quad (3)$$

Ignoring the anti-resonant terms, and making the rotating-wave transformation, we get the hamiltonian for the system:

$$H = \frac{\hbar}{2} \begin{bmatrix} \Delta & 0 & -g_1(z) \\ 0 & -\Delta & -g_2(z) \\ -g_1(z) & -g_2(z) & -2\delta \end{bmatrix} \\ = (\hbar/2) [ \Delta (|a\rangle\langle a| - |b\rangle\langle b|) - 2\delta |c\rangle\langle c| - g_1(z) (|a\rangle\langle c| + \text{h.c.}) - g_2(z) (|b\rangle\langle c| + \text{h.c.}) ] . \quad (4)$$

Here, the Rabi frequencies are real, and the common detuning  $\delta$  and the difference detuning  $\Delta$  are as defined in fig. 1b. In what follows, we will consider primarily the case where  $\Delta=0$ . We also assume that states  $|a\rangle$  and  $|b\rangle$  are degenerate, so that  $\omega_1 = \omega_2 \equiv \omega$ ,  $\delta_1 = \delta_2 \equiv \delta$ , and  $k_1 = k_2 \equiv k$ . In addition, for simplicity we consider only the case of  $g_{10} = g_{20} \equiv 4g$ .

So far, we have assumed that  $z$ , the position of the center of mass of the atom, can be treated as a classical

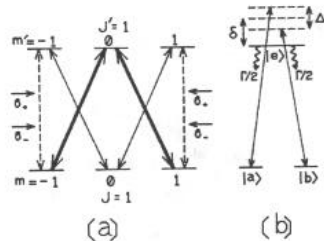


Fig. 1. (a) A  $J=1 \leftrightarrow J'=1$  transition, excited by a pair of circularly polarized standing waves. (b) The resulting ideal  $\Lambda$  system:  $\delta$  is the average detuning,  $\Delta$  is the differential detuning, and  $\Gamma$  is the excited state decay rate.

variable. However, we want to allow for the possibility that the atoms become cold enough that the de Broglie wavelengths become comparable to or bigger than the optical wavelength [6]. In this regime, it is necessary to treat  $z$  as a quantum mechanical operator,  $\hat{z}$ , with the atom's linear momentum in the  $z$ -direction,  $\hat{p}$ , being the canonical conjugate. Denoting by  $|p\rangle$  the eigenstate of  $\hat{p}$  (i.e.,  $\hat{p}|p\rangle = p|p\rangle$ ), the basis states can now be written as

$$|a, p_a\rangle \equiv |a\rangle \otimes |p_a\rangle, \quad |b, p_b\rangle \equiv |b\rangle \otimes |p_b\rangle, \quad |c, p_c\rangle \equiv |c\rangle \otimes |p_c\rangle, \quad (5)$$

where the linear momentum is a continuous variable:  $-\infty < p_i < \infty$ , ( $i = a, b, c$ ). In order to find the hamiltonian in this basis, we note first that

$$\exp(\pm ik\hat{z}) = \int_{-\infty}^{+\infty} dp |p\rangle \langle p \mp \hbar k|, \quad (6)$$

which simply means that a travelling wave optical field with a wavenumber  $k$  couples a state with a momentum  $p - \hbar k$  to a state with a momentum  $p$ , conserving linear momentum. Given eq. (6), and noting that the kinetic energy of a state  $|p\rangle$  is  $p^2/2M$ , where  $M$  is the mass of the atom, we get the following form for the hamiltonian:

$$\begin{aligned} H = & \sum_{p_a, p_b, p_c} \left[ \frac{p_a^2}{2M} |a, p_a\rangle \langle a, p_a| + \frac{p_b^2}{2M} |b, p_b\rangle \langle b, p_b| + \left( \frac{p_c^2}{2M} - \hbar\delta \right) |c, p_c\rangle \langle c, p_c| \right] \\ & - \hbar g \int_{-\infty}^{+\infty} dp (|p\rangle \langle p + \hbar k| + |p\rangle \langle p - \hbar k|) (|a\rangle \langle c| + \text{h.c.}) \\ & - \hbar g \int_{-\infty}^{+\infty} dp [ |p\rangle \langle p + \hbar k| \exp(-i\phi) + |p\rangle \langle p - \hbar k| \exp(i\phi) ] (|b\rangle \langle c| + \text{h.c.}) . \end{aligned} \quad (7)$$

To illustrate this, consider some representative matrix elements. For example, the energy of the state  $|a, p_a\rangle$  is given by  $\langle a, p_a | H | a, p_a \rangle = p_a^2/2M$ , while the coupling between states  $|a, p_a\rangle$  and  $|c, p_c\rangle$  is given by

$$\langle a, p_a | H | c, p_c \rangle = -\hbar g [\delta_{p_a, p_c - \hbar k} + \delta_{p_a, p_c + \hbar k}], \quad \delta_{i,j} = 0 \text{ if } i \neq j \text{ and } 1 \text{ if } i = j. \quad (8)$$

This hamiltonian is illustrated in fig. 2 for a few of the infinite number of basis states. As can be seen, each of the ground states is connected to two excited states. Therefore, it is not possible to find closed families of states, as is possible for two travelling waves. Nevertheless, we will be able to find a velocity selective dark state and calculate the VSCPT rate into this state (as a function of  $\phi$ ) both perturbatively and by numerically integrating the optical Bloch equations [6].

In analogy to the travelling wave VSCPT, we are interested in finding a state (the dark state) which satisfies the following conditions: (i) it does not contain any excited state, so that it is completely decoupled from the vacuum fields, and (ii) the net amplitude for coupling this state to any of the excited states must vanish. It can be shown that if  $p=0$  and/or  $\phi=0$  then the state

$$|NC(p)\rangle = \frac{1}{2} [ |a, p - \hbar k\rangle \exp(-i\phi) + |a, p + \hbar k\rangle \exp(i\phi) - |b, p - \hbar k\rangle - |b, p + \hbar k\rangle ] \quad (9)$$

does not couple to any excited state. This is illustrated in fig. 3 for two cases:  $p=0$  (levels denoted by solid lines) and  $p \neq 0$  (levels denoted by dashed lines). In either case, momentum conservation allows for only three excited states to be coupled by the hamiltonian directly to  $|NC(p)\rangle$ . We will show that the coupling to each of these states vanishes (for  $p=0$  and/or  $\phi=0$ ) by showing that if the system is in the state  $|NC\rangle$  at  $t=0$ , then it remains in  $|NC\rangle$  after an infinitesimal amount of time,  $dt$ .

We introduce the following notation for the seven levels of fig. 3:

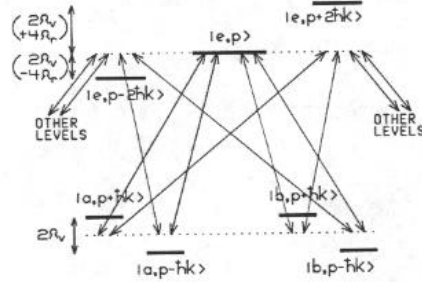


Fig. 2. Illustration of the energy levels of and couplings between a typical set of momentum states in a  $\Lambda$  system excited by standing wave fields. Here, we have chosen  $\delta = -\Omega_r$ .

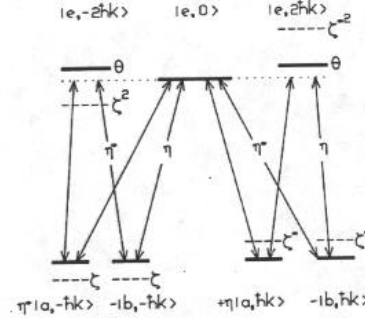


Fig. 3. Illustration of the dark state,  $|NC(0)\rangle$  (levels denoted by solid lines) and the state  $|NC(p)\rangle$  (levels denoted by dashed lines). Here,  $\eta = \exp(i\phi)$ ,  $\theta = \exp(i4\Omega_r t)$ , and  $\zeta = \exp(i\Omega_r t)$ . The energy zero is chosen to be  $(p^2)/(2M)$ . Note that this causes overlap of the states  $|e, p\rangle$  and  $|e, 0\rangle$ . The symbols in the transition lines represent the effects of the standing wave phase shift, whereas those next to the solid ( $p=0$ ) levels are associated with the phases produced by the motional energy shifts. The symbols next to the dashed ( $p \neq 0$ ) levels are the additional phases associated with the center-of-mass momentum,  $p$ . Finally, the weights for the state  $|NC\rangle$  are shown to the ground state labels.

$$\begin{aligned} |1\rangle &\equiv |a, p - \hbar k\rangle, \quad |2\rangle \equiv |a, p + \hbar k\rangle, \quad |3\rangle \equiv |b, p - \hbar k\rangle, \quad |4\rangle \equiv |b, p + \hbar k\rangle, \\ |5\rangle &\equiv |e, p - 2\hbar k\rangle, \quad |6\rangle \equiv |e, p\rangle, \quad |7\rangle \equiv |e, p + 2\hbar k\rangle. \end{aligned} \quad (10)$$

The wave function<sup>#2</sup> can be written as

$$|\psi\rangle = \sum_i A_i |i\rangle, \quad i = 1, 2, \dots, 7. \quad (11)$$

The reduced hamiltonian for this subset of states is given, from eq. (7) by

$$H = \hbar \begin{bmatrix} -\Omega_v & 0 & 0 & 0 & g & g & 0 \\ 0 & \Omega_v & 0 & 0 & 0 & g & g \\ 0 & 0 & -\Omega_v & 0 & g\eta^* & g\eta & 0 \\ 0 & 0 & 0 & \Omega_v & 0 & g\eta^* & g\eta \\ g & 0 & g\eta & 0 & -2\Omega_v + 4\Omega_r & 0 & 0 \\ g & g & g\eta^* & g\eta & 0 & 0 & 0 \\ 0 & g & 0 & g\eta^* & 0 & 0 & 2\Omega_v + 4\Omega_r \end{bmatrix}. \quad (12)$$

Here, denoting by  $v$  the velocity corresponding to the momentum  $p$ , we define the Doppler shift,  $\Omega_v \equiv Pk/m = kv$ , the recoil energy,  $\Omega_r \equiv \hbar k^2/2M$ , and  $\eta \equiv \exp(i\phi)$ . Note that for simplicity, we have chosen  $\delta = -\Omega_r$ , and have shifted the zero of energy to coincide with the energy of state  $|6\rangle$ .

<sup>#2</sup> The use of wave function is exactly valid for the case where  $|NC\rangle$  is a dark state, which implies that  $A_3 = A_4 = A_7 = 0$  for  $t \geq 0$ . When  $|NC\rangle$  is not a dark state, the wave function approach is still valid as long as  $dt \ll 1/T$ .

Note now that the dark state,  $|\text{NC}(p)\rangle$ , is a linear combination of states  $|1\rangle$  through  $|4\rangle$ . We define  $|C_1(p)\rangle$ ,  $|C_2(p)\rangle$  and  $|C_3(p)\rangle$  as three other mutually orthogonal states such that

$$\begin{bmatrix} |\text{NC}\rangle \\ |C_1\rangle \\ |C_2\rangle \\ |C_3\rangle \end{bmatrix} = \frac{1}{2} \begin{bmatrix} \eta^* & \eta & -1 & -1 \\ \eta^* & -\eta & 1 & -1 \\ \eta^* & \eta & 1 & 1 \\ -\eta^* & \eta & 1 & -1 \end{bmatrix} \begin{bmatrix} |1\rangle \\ |2\rangle \\ |3\rangle \\ |4\rangle \end{bmatrix}. \quad (13)$$

The wavefunction can now be written as

$$|\psi\rangle = A_{\text{NC}} |\text{NC}\rangle + A_{c_1} |C_1\rangle + A_{c_2} |C_2\rangle + A_{c_3} |C_3\rangle + A_5 |5\rangle + A_6 |6\rangle + A_7 |7\rangle. \quad (14)$$

Using eqs. (12) and (13), we get the hamiltonian for this basis:

$$H = \hbar \begin{bmatrix} 0 & 0 & 0 & \Omega_v & 0 & 0 & 0 \\ 0 & 0 & -\Omega_v & 0 & g\eta^* & 0 & -g\eta \\ 0 & -\Omega_v & 0 & 0 & g\eta^* & 2Cg & g\eta \\ \Omega_v & 0 & 0 & 0 & 0 & i2Sg & 0 \\ 0 & g\eta & g\eta & 0 & 2(2\Omega_v - \Omega_v) & 0 & 0 \\ 0 & 0 & 2Cg & -i2Sg & 0 & 0 & 0 \\ 0 & -g\eta^* & g\eta^* & 0 & 0 & 0 & 2(2\Omega_v + \Omega_v) \end{bmatrix}. \quad (15)$$

Here, we have defined  $S \equiv \sin \phi$  and  $C \equiv \cos \phi$  so that  $\eta = C + iS$ .

For  $p=0$ , so that  $\Omega_v=0$ , it is clear from eq. (15) that the state  $|\text{NC}(0)\rangle$  is completely decoupled from any state. Therefore,  $|\text{NC}(0)\rangle$  is a pure dark state. For  $p \neq 0$ , consider first the case of  $\phi \neq n\pi$ , where  $n$  is an integer. Note that  $|\text{NC}(p)\rangle$  is still not coupled directly to any of the excited states. However, it is coupled to  $|C_3(p)\rangle$ , which in turn is coupled to one of the excited states,  $|6(p)\rangle$ . Thus, for  $\phi \neq n\pi$ , atoms with non-zero velocity will be optically pumped into  $|\text{NC}(0)\rangle$ , which is the zero velocity dark state. This is of course velocity selective coherent population trapping (VSCPT).

Consider next the case of  $\phi = n\pi$ , with  $p \neq 0$ . In this case,  $S = \sin \phi = 0$ , so that  $|\text{NC}(p)\rangle$  is coupled only to  $|C_3(p)\rangle$ , which in turn is coupled only to  $|\text{NC}(p)\rangle$ . Thus, both  $|\text{NC}(p)\rangle$  and  $|C_3(p)\rangle$  are pure trapped states, independent of the value of  $p$ , as long as  $\phi = n\pi$ . Since there are pure trapped states at each velocity, VSCPT does not take place when  $\phi = n\pi$ .

To see how the efficiency of VSCPT depends on  $\phi$ , it is necessary to determine the net coupling rate  $|\text{NC}(p)\rangle$  to the excited state  $|6(p)\rangle$  via the state  $|C_3(p)\rangle$ . By formal integration, we can write

$$A_6(t) = \int_0^t dt' \int_0^{t'} dt'' \ddot{A}_6(t''). \quad (16)$$

In the perturbative limit, where at  $t=0$  all the atoms are in the state  $|\text{NC}\rangle$ , the integrand can be found from applying the Schrodinger equation twice:

$$\ddot{A}_6(t'') = (-i/\hbar)^2 \langle \text{NC} | H | C_3 \rangle \langle C_3 | H | 6 \rangle A_{\text{NC}}(t''). \quad (17)$$

Since the hamiltonian is independent of time, and  $A_{\text{NC}}(t'') \approx 1$  is a constant in the perturbative limit, we find that the amplitude of the state  $|6\rangle$  after a differential amount of time,  $dt$ , is given by

$$dA_6(p) = (dt)^2 (-i/\hbar)^2 \langle \text{NC} | H | C_3 \rangle \langle C_3 | H | 6 \rangle = -2i(dt)^2 \Omega_v g \sin \phi = -2i(dt)^2 (p/m) kg \sin \phi. \quad (18)$$

Thus, the net rate at which atoms starting in  $|\text{NC}(p)\rangle$  is coupled into the excited state is proportional to  $(p \sin \phi)^2$ .

The formal approach used in deriving eq. (18) is presented to clarify the physics of VSCPT in standing

waves, as well as to demonstrate the existence of additional dark states when  $\phi=0$ . However, it is possible to understand the behavior in eq. (18) in a relatively simple way by inspection of fig. 3. If  $p \neq 0$  (the dashed levels in the figure), each level has an additional energy due to the kinetic energy associated with the momentum. In the figure, the energy  $p^2/2M$  is chosen as the energy zero so that the states  $|e, 0\rangle$  and  $|e, p\rangle$  are superimposed. If we consider the sum of the interaction matrix elements coupling the ground states to each of the excited states, we see that the couplings to the levels  $|e, p-2\hbar k\rangle$  and  $|e, p+2\hbar k\rangle$  still vanish but the coupling to the level  $|e, p\rangle$  does not. In particular, assume that the atoms are in  $|NC\rangle$  at  $t=0$ , as given by eq. (9). The problem now becomes one of weighted summation of the four transition paths to state  $|e, p\rangle$  from the ground states, as shown in fig. 3. Using the relative ground state weights (shown in fig. 3) and the relative transition matrix elements we find that

$$\langle e, p | NC(p) \rangle \propto [\eta^* \zeta + \eta \zeta^* - \eta \zeta - \eta^* \zeta^*] \propto \sin(\Omega_v t) \sin \phi. \quad (19)$$

Note that since  $\eta = \exp(i\phi)$  and  $\zeta = \exp(i\Omega_v t)$ , eq. (19) has the same functional dependence on  $\phi$  and  $\Omega_v$  as eq. (18), in the limit of small  $t$ . Thus, the expression for the efficiency of VSCPT can be derived essentially by inspection of fig. 3.

According to eq. (19), we expect that the efficiency of VSCPT would vary roughly as  $\sin^2 \phi$ , being maximum at  $\phi = (2n+1)\pi/2$  and vanishing at  $\phi = n\pi$ . This phase dependence of standing wave VSCPT is also consistent with the semi-classical picture. Consider the basis states  $|-\rangle = \cos \theta |a\rangle - \sin \theta |b\rangle$ ,  $|+\rangle = \sin \theta |a\rangle + \cos \theta |b\rangle$ , and  $|e\rangle$  where  $\theta(v) = \tan^{-1}[g_1(v)/g_2(v)]$ . For  $v=0$ ,  $g_1$  and  $g_2$  are constants, and the  $|-\rangle$  state is the dark state, decoupled from  $|+\rangle$  and  $|e\rangle$ . For  $v \neq 0$ ,  $|-\rangle$  is coupled to  $|+\rangle$  at the rate of  $v \nabla \theta \propto kv \sin \phi$ . Note that the phase dependence of this coupling rate is also the same as the phase dependence of VSCPT (eqs. (18) and (19)) since  $\Omega_v = kv$ . In particular, for  $\phi=0$ ,  $g_1=g_2$  at all positions and therefore  $\theta(v)$  is a constant, so that this coupling vanishes, and  $|-\rangle$  is a dark state for each velocity.

It is also possible to estimate the relative efficiency of standing wave VSCPT compared to that of travelling wave VSCPT. Consider the case of  $\phi = (2n+1)\pi/2$ . In this case,  $|NC(p)\rangle$  is coupled to  $|C_3(p)\rangle$  at the rate of  $\Omega_v$ . In turn, states  $|C_1(p)\rangle$ ,  $|C_2(p)\rangle$ ,  $|C_3(p)\rangle$  are each coupled to the excited state (through one or more channels) at the rate of  $2g$ , as given by eq. (15). If we analyze the travelling wave case in the same way, we find that the coupling rates are the same, except that there are only three states,  $(|a, p-\hbar k\rangle - |b, p+\hbar k\rangle)$ ,  $(|a, p-\hbar k\rangle + |b, p+\hbar k\rangle)$  and  $|e, p\rangle$ , which have properties analogous to  $|NC\rangle$ ,  $|C_3\rangle$ , and  $|6\rangle$ , respectively. Thus, for  $\phi = (2n+1)\pi/2$ , we expect the standing wave VSCPT efficiency to be of the same order of magnitude as the travelling wave VSCPT efficiency.

The VSCPT rate derived above (eq. (18)) is in agreement with numerical simulations obtained by integrating the optical Bloch equations for the  $\Lambda$  system under standing wave excitation. In particular, we calculated the time evolution of the momentum distribution for different values of  $\phi$ . Even though there are no closed families of states in the SW system, an excited state with momentum  $p$  is still coupled only to ground states with momenta  $p \pm \hbar k$  which in turn couple to excited states with momenta  $p \pm 2\hbar k$ , etc. Thus, there are still families of states which can be closed by truncation. For our calculation, we choose a momentum range of  $\pm 5\hbar k$ .

Figure 4 shows the initial (top trace) and final momentum distributions at  $t=50\Gamma^{-1}$  for helium excited by standing waves of the phase indicated (middle traces), and also for travelling wave excitation (bottom trace), included for comparison. We see that for  $\phi=\pi/2$  VSCPT does occur and is about half as efficient as for travelling waves. For other  $\phi$ , we see the predicted  $\sin^2 \phi$  dependence. In particular, at  $\phi=0$  there is no peaking of the momentum distribution<sup>#3</sup>.

<sup>#3</sup> In fact, we see some very slight alteration in the momentum distribution at  $\phi=0$  due to optical pumping into the relevant dark states. However, after a short time ( $<50\Gamma^{-1}$ ) the momentum redistribution stops, in contrast to the  $\phi \neq 0$  cases where the  $\pm \hbar k$  peaks continue to grow and sharpen.

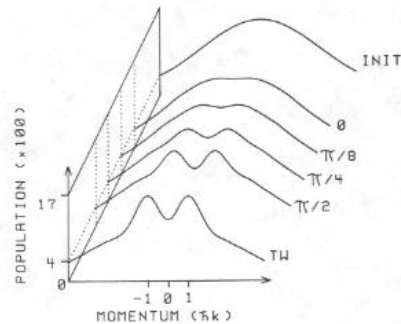


Fig. 4. Numerical simulation of VSCPT in the  $\Lambda$  system with standing waves after  $t = 50\Gamma^{-1}$  for He, where  $g_{10} = g_{20} = 0.3\Gamma$  and  $\delta = \Delta = 0$ . INIT is the initial momentum distribution: a gaussian distribution in the ground states with a standard half width at  $e^{-1/2}$  of  $3\hbar k$ . The middle 4 traces are for standing wave excitation with the phases  $\phi$  as indicated. TW is travelling wave case with Rabi frequencies  $g_{\sigma+} = g_{\sigma-} = 0.3\Gamma$ . In all cases, momentum is in units of  $\hbar k$  and population is normalized to 1.

### 3. Previous experimental evidence of standing wave VSCPT

As mentioned earlier, both the existence and the approximate phase dependence of one dimensional VSCPT in Raman resonant standing waves have already been observed by Aspect et al. [1], for the  $j=1 \leftrightarrow j'=1$  transition in metastable helium. However, since these results were not explicitly presented in the context of standing wave phase shifts, we will now review these observations for completeness. In the first part of the Aspect experiment, VSCPT was observed as a pair of peaks in the momentum distribution when the  $\text{He}^*$  beam was excited with a pair of counterpropagating laser beams having opposite circular polarizations. For the  $\Lambda$  system in the  $j=1 \leftrightarrow j'=1$  transition this is of course equivalent to a pair of counter-propagating pure travelling waves. In the second part of the experiment, the  $\text{He}^*$  beam was excited by counter-propagating linearly polarized laser beams where the polarization axes of the forward and backward propagating laser beams had a relative angle of  $\chi$ . Specifically,  $\chi=0$  and  $\chi=\pi/2$  correspond respectively to the so-called lin-parallel-lin and lin-perp-lin configuration. It is easy to show that for the  $j=1 \leftrightarrow j'=1$  transition these experimental configurations are equivalent to a pair of opposite-circularly polarized Raman resonant standing waves, having a phase shift  $\phi=\chi$ . As reported, no VSCPT was observed when  $\chi=0$ , but the double peaked momentum distribution reappeared (as evidence of VSCPT) when  $\chi=\pi/2$ . This is in agreement with the present theory. In addition, the relative peak heights in the Aspect experiment are consistent (within experimental noise) with our theoretical prediction of relative efficiencies in fig. 4.

Here, it must be acknowledged that for the specific case of the  $j=1 \leftrightarrow j'=1$  transition, Kaiser et al. [7] correctly explained the presence of VSCPT for the lin-perp-lin case and the absence thereof for the lin-parallel-lin case by considering transitions between superpositions of the magnetic sublevels forming closed families of states for this system. However, we emphasize that the theory presented in this paper is not limited to the  $j=1 \leftrightarrow j'=1$  transition, and is valid for any pair of Raman resonant standing waves exciting a  $\Lambda$  system. In addition, our analysis gives the detailed phase dependence of VSCPT efficiency. This is important in the context of a stimulated Raman trap, since both the deflecting force and the pol-grad cooling force are maximum at  $\phi=\pi/4$  and vanish [3] at  $\chi=0$  and  $\chi=\pi/2$ .

### 4. Generalization to three dimensions

Finally, we have found [3] that this process can be generalized to three dimensions. Briefly, the scheme again

employs a  $j=1 \leftrightarrow j'=1$  transition, except with three mutually orthogonal pairs of Raman resonant standing waves having direction vectors  $\hat{x}$ ,  $\hat{y}$  and  $\hat{z}$ . This is accomplished using left-circularly polarized and right-circularly polarized standing waves, with phase differences of  $\phi_i$ ,  $i=x, y, z$ . Under this configuration, VSCPT takes place into a zero velocity three-dimensional dark state of the form  $\psi = A_+ |m_z = +1\rangle + A_0 |m_z = 0\rangle + A_- |m_z = -1\rangle$ , where  $A_+$ ,  $A_0$ , and  $A_-$  are the standing wave field amplitudes at each point in space, which comprise of summations over momentum eigenstates. Note that the mathematical form of this zero velocity three-dimensional dark state is similar to that found by Ol'shanii et al. [8], except that standing waves (rather than travelling waves) are used in the present case. To compute the efficiency of VSCPT in three dimensions, it is necessary to consider other states with non-zero net momentum as well. Extrapolation of the one dimensional analysis suggests that this would yield a VSCPT efficiency as a complicated function of  $\phi_x$ ,  $\phi_y$ , and  $\phi_z$ , and the analysis have not yet been performed. Note that there is no phase dependence in the travelling wave three-dimensional VSCPT considered by Ol'shanii et al. [8].

### 5. Summary

We have shown theoretically that phase sensitive VSCPT takes place when a  $\Lambda$  system is excited by a pair of Raman resonant standing waves. This corresponds to absence of diffusion for zero velocity atoms in the trapped state. We also review previous experimental observations reported by Aspect et al. which agree with our predictions. Finally, we outline the generalization to three dimensions. Given our prior observation of stimulated trapping and cooling forces and our theoretical prediction of strong pol-grad cooling in Raman resonant standing waves, the simultaneous existence of VSCPT may make it possible to design a subrecoil temperature trap for  $\Lambda$  atoms.

### Acknowledgements

We wish to acknowledge the helpful discussions with Prof. S. Ezekiel of MIT, and A. Aspect and R. Kaiser of Institut d'Optique Théorique et Appliquée. This work was supported by Rome Laboratory Contract No. F19628-92-K-0013 and Office of Naval Research Grant No. ONR-N0014-91-HJ-1808. NPB is an Alfred P. Sloan Research Fellow.

### References

- [1] A. Aspect, E. Arimondo, R. Kaiser, N. Vansteenkiste and C. Cohen-Tannoudji, *Phys. Rev. Lett.* 61 (1988) 826.
- [2] F. Mauri and E. Arimondo, *Appl. Phys. B* 54 (1992) 2408.
- [3] M.S. Shahriar, P.R. Hemmer, M.G. Prentiss, J. Mervis, D.P. Katz, T. Cai and N. Bigelow, *Bulletin of the American Physical Society, Series II*, Vol. 38, No. 3, p. 1122 (1993), presented in the 1993 Annual Meeting of the Division of Atomic, Molecular, and Optical Physics, Reno, NV, 1993; P. Hemmer, M. Shahriar, M. Prentiss, D. Katz, K. Berggren, J. Mervis and N. Bigelow, *Bulletin of the American Physical Society, Series II*, Vol. 37, No. 4, p. 1208 (1992) presented in the Interdisciplinary Laser Science Conf., Albuquerque, NM, 1992.
- [4] P. Hemmer, M. Shahriar, M. Prentiss, D. Katz, K. Berggren, J. Mervis and N. Bigelow, *Phys. Rev. Lett.* 68 (1992) 3148.
- [5] S. Chang, B. Garraway and V. Minogin, *Optics Comm.* 77 (1990) 19.
- [6] A. Aspect, E. Arimondo, R. Kaiser, N. Vansteenkiste and C. Cohen-Tannoudji, *J. Opt. Soc. Am. B* 6 (1989) 2112.
- [7] R. Kaiser, *These de Doctorat, Ecole Normale Supérieure*, 1990 (unpublished).
- [8] M. Ol'shanii and V. Minogin, *Proc. Int. Workshop on Light induced kinetic effects on atoms, ions, and molecules*, Marciana Marina, Italy, eds. L. Moi et al. (ETS Editrice, Pisa, 1991) p. 99.